Decorin causes autophagy in endothelial cells via Peg3

Simone Buraschi[a,b,1], Thomas Neill[a,b,1], Atul Goyal[a,b], Chiara Poluzzi[a,b], James Smythies[a,b], Rick T. Owens[c], Liliana Schaefer[d], Annabel Torres[a,b], and Renato V. Iozzo[a,b,2]

[a]Department of Pathology, Anatomy and Cell Biology, and the [b]Cell Biology and Signaling Program, Kimmel Cancer Center, Thomas Jefferson University, Philadelphia, PA 19107; [c]LifeCell Corporation, Branchburg, NJ 08876; and [d]Pharmazentrum Frankfurt, Goethe University, 60590 Frankfurt, Germany

Edited by Carlo M. Croce, The Ohio State University, Columbus, Ohio, and approved May 29, 2013 (received for review March 27, 2013)

Soluble decorin affects the biology of several receptor tyrosine kinases by triggering receptor internalization and degradation. We found that decorin induced paternally expressed gene 3 (*Peg3*), an imprinted tumor suppressor gene, and that Peg3 relocated into autophagosomes labeled by Beclin 1 and microtubule-associated light chain 3. Decorin evoked Peg3-dependent autophagy in both microvascular and macrovascular endothelial cells leading to suppression of angiogenesis. Peg3 coimmunoprecipitated with Beclin 1 and LC3 and was required for maintaining basal levels of Beclin 1. Decorin, via Peg3, induced transcription of Beclin 1 and microtubule-associated protein 1 light chain 3 alpha genes, thereby leading to a protracted autophagic program. Mechanistically, decorin interacted with VEGF receptor 2 (VEGFR2) in a region overlapping with its natural ligand VEGFA, and VEGFR2 was required for decorin-evoked Beclin 1 and microtubule-associated protein 1 light chain 3 alpha expression as well as for Peg3 induction in endothelial cells. Moreover, decorin induced VEGFR2-dependent mitochondrial fragmentation and loss of mitochondrial membrane potential. Thus, we have unveiled a mechanism for a secreted proteoglycan in inducing Peg3, a master regulator of macroautophagy in endothelial cells.

small leucine-rich proteoglycan | microvascular endothelial cells | porcine aortic endothelial cells

The molecular and cellular biology of the tumor stroma is now becoming a prominent theme of research in tumor promotion and progression (1). Decorin is a secreted proteoglycan that belongs to a multifunctional family of proteoglycans collectively designated as small leucine-rich proteoglycans (SLRPs) (2). Many SLRPs, including decorin and biglycan, regulate a variety of vital biological processes, especially via their innate ability to bind collagen type I and ultimately regulate fibrillogenesis and bioavailability of various growth factors (3). However, many recent studies have broadened our view of decorin from a specialized collagen-bound factor and regulator of matrix assembly to that of a soluble multifunctional signaling proteoglycan (4, 5). For example, circulating decorin has been detected in the plasma of normal volunteers and found to be elevated in diabetic (6) and septic patients (7). In contrast, decreased plasma levels of decorin have been detected in acute ischemic stroke (8) and in patients with esophageal squamous cell carcinomas (9). Plasma levels of decorin can range between 8 and 80 ng/mL, a reasonable level capable of evoking signaling in target organs. Furthermore, decorin can be synthesized de novo by macrophages during septic and aseptic inflammatory responses (7).

Soluble decorin (10) now is emerging as a pan-receptor tyrosine kinase inhibitor and has a broad binding repertoire with various growth factors and a multitude of cell-surface receptors (11–15). Based on these unique features, we have proposed that decorin could be considered a "guardian from the matrix" in analogy to p53, which is referred to as the "guardian of the genome" (16). Our main hypothesis is that decorin functions as an endogenous soluble inhibitor of cancer growth and angiogenesis (17–21). Collectively, these properties are critical for decorin to act as a potent tumoricidal agent, as demonstrated conclusively by systemically administered decorin labeled with IR-Dye 800 avidly, specifically, and stably targeting orthotopic tumor xenografts (22). Moreover, decorin is capable of significantly inhibiting neovascularization of triple-negative basal cell breast carcinomas (23).

During preclinical studies focusing on identifying decorin-induced genes in vivo, we found that systemic delivery of decorin protein core to mice carrying orthotopic mammary carcinoma xenografts induced expression of a small subset of genes (24). Notably, these genes were induced exclusively in the tumor stroma of mouse origin but not in the mammary carcinomas of human origin (24). One of the most up-regulated genes was Paternally expressed gene 3 (*Peg3*), an imprinted putative tumor-suppressor gene frequently silenced by promoter hypermethylation and/or loss of heterozygosity (25–30). Interestingly, Peg3 binds β-catenin and promotes 26S proteasomal degradation that is, surprisingly, independent of glycogen synthase kinase-3β GSK3β (31). Because Peg3 activity phenocopies the pathway used by decorin for the noncanonical, GSK3β-independent antagonism and cessation of β-catenin signaling (22), we hypothesized that decorin-induced Peg3 could cooperate with decorin in inducing stromal-specific changes in the context of tumor angiogenesis. In this study we discovered that decorin-induced Peg3 promoted the expression of autophagic proteins such as Beclin 1 and light chain 3 (LC3) in endothelial cells and that Peg3 interacted directly with Beclin 1, LC3, and β-catenin. In addition to to these protein–protein interactions, we also discovered a critical role for Peg3 in regulating decorin-evoked expression of these canonical autophagic markers specifically within endothelial cells. This biological activity of decorin was mediated primarily by an interaction with VEGF receptor 2 (VEGFR2), and its tyrosine kinase activity was required for induction of autophagic genes in both macro- and microvascular endothelial cells. Our study provides evidence that a soluble constituent of the extracellular matrix can affect the intracellular digestive machinery and firmly establishes Peg3 as a master regulator of macroautophagy.

Significance

We identified a function for a member of the extracellular matrix in the regulation of autophagy. Decorin, a member of the small leucine-rich proteoglycan family and an established pan-receptor tyrosine kinase inhibitor, evokes endothelial cell autophagy and inhibits angiogenesis. This process is mediated by a high-affinity interaction with VEGFR2 which leads to increased levels of Peg3, a tumor-suppressor gene. We provide mechanistic evidence that Peg3 is required to maintain basal levels of Beclin 1, a major autophagic marker. These data provide a paradigmatic shift for other soluble matrix constituents to regulate autophagy.

Author contributions: S.B., T.N., A.G., C.P., J.S., A.T., and R.V.I. designed research; S.B., T.N., A.G., C.P., J.S., A.T., and R.V.I. performed research; R.T.O. contributed new reagents/analytic tools; L.S. analyzed data; and T.N. and R.V.I. wrote the paper.

The authors declare no conflict of interest.

This article is a PNAS Direct Submission.

[1]S.B. and T.N. contributed equally to this work.

[2]To whom correspondence should be addressed. E-mail: renato.iozzo@jefferson.edu.

This article contains supporting information online at www.pnas.org/lookup/suppl/doi:10.1073/pnas.1305732110/-/DCSupplemental.

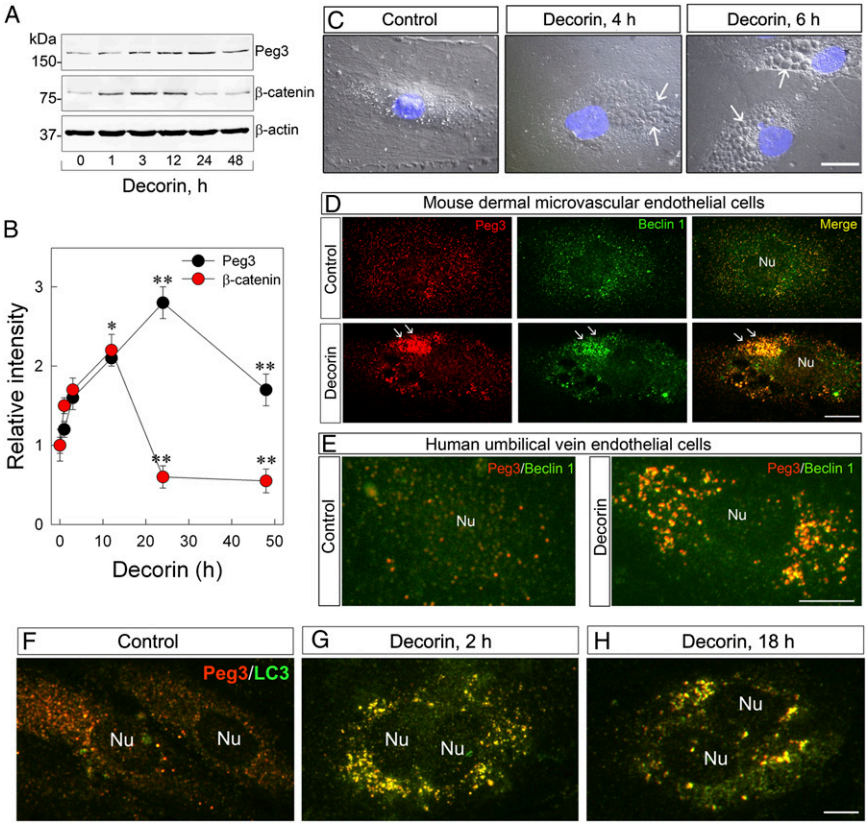

Fig. 1. Decorin up-regulates the levels of Peg3 in endothelial cells and causes its redistribution and colocalization with Beclin 1 and LC3 in large autophagosomes. (*A*) Representative Western blot showing induction of Peg3 and transient induction and subsequent down-regulation of β-catenin protein levels in HUVEC treated with 200 nM decorin at the indicated time points. β-Actin served as loading control. (*B*) Quantification of the protein levels of Peg3 and β-catenin, respectively, from four independent experiments; data are shown as mean ± SEM. $*P < 0.05$; $**P < 0.01$. (*C*) Representative DIC/fluorescence images of MDEC treated with 200 nM decorin for 4 and 6 h. White arrows indicate autophagosomes fully formed in the cytoplasm of the cells upon exposure to decorin. Nuclei were stained with DAPI. The images shown are representative of three independent experiments. (Scale bar: ~10 μm.) (*D* and *E*) Confocal (*D*) and fluorescence (*E*) images of Peg3 and Beclin 1 cellular colocalization in MDEC and HUVEC, respectively, upon a 6-h treatment with 200 nM decorin. Nu, nucleus. (Scale bar: ~8 μm.) (*F–H*) Representative fluorescence images of HUVEC after 2- and 18-h incubation with 200 nM decorin stained for Peg3 and LC3 as indicated. Images are representative of several independent experiments (n = 4–5). Nu, nucleus. (Scale bar: ~6 μm.)

Results

Decorin Evokes Concurrent Induction of Peg3 and Autophagy in Endothelial Cells. Because the newly formed microcirculation is a key component of the tumor stroma, we tested whether decorin could directly induce expression of Peg3 in human umbilical vein endothelial cells (HUVEC) and in mouse microvascular dermal endothelial cells (MDEC). We discovered that decorin protein core (herein referred to as decorin) induced Peg3 expression in a time-dependent fashion in HUVEC (Fig. 1*A*). Unlike human fibroblasts, HUVEC and porcine aortic endothelial cells that overexpress VEGFR-2 (PAE-VEGFR2) do not express endogenous decorin, as evaluated by quantitative real-time PCR (qPCR) (Fig. S1*A*). Furthermore, *VEGFA* mRNA was increased approximately sixfold in PAE-VEGFR2 cells relative to human fibroblasts and HUVEC, as is consistent with VEGFR2 driving *VEGFA* expression (Fig. S1*A*). Thus, the results presented here are not confounded by endogenous decorin production by endothelial cells. Quantification of four independent experiments showed that Peg3 levels were induced rapidly and remained elevated for up to 48 h ($P < 0.01$) (Fig. 1*B*). In contrast, decorin caused a transient up-regulation of β-catenin (Fig. 1*A*), which peaked at 12 h and subsequently declined below basal levels for up to 48 h ($P < 0.01$, Fig. 1*B*). Thus, decorin dynamically regulates Peg3 and β-catenin levels in endothelial cells.

We performed differential interference contrast (DIC) microscopy and discovered that 4- to 6-h exposure to decorin induced numerous cytoplasmic vacuoles reminiscent of autophagosomes (white arrows, Fig. 1*C*). We next performed immunofluorescence microscopy using antibodies for Peg3 and Beclin 1, a major autophagic marker (32). Decorin evoked redistribution of Peg3 from a diffusely punctuate cytoplasmic location to autophagosomes as shown by Peg3 colocalization with Beclin 1 in both MDEC (Fig. 1*D*) and HUVEC (Fig. 1*E*). Surface plots also indicated induction of both Peg3 (Fig. S1*B*) and Beclin 1 (Fig. S1*C*) in MDEC. We found no difference in bioactivity when using decorin proteoglycan, because induction still occurred for Peg3 (Fig. S1*D*) and Beclin 1 (Fig. S1*E*).

To corroborate the evidence of vesicular autophagy, we immunostained both MDEC and HUVEC with an antibody specific for microtubule-associated LC3. LC3, a well-characterized biomarker of autophagy, normally is localized to the cytosol, but during autophagy it is lipidated and becomes membrane bound (32). We found that, like Beclin1, Peg3 and LC3 colocalized to large vacuoles in HUVEC treated with decorin (Fig. 1 *G* and *H*), in contrast to vehicle-treated cells (Fig. 1*F*), further supporting the concept that Peg3 might be directly related to autophagy.

For further proof of decorin-evoked autophagy, we performed ultrastructural analysis following 18-h treatment with decorin (200 nM). The number of vesicular structures was markedly increased in MDEC (arrows, Fig. 2*B*) compared with vehicle-treated cells (Fig. 2*A*). Importantly, numerous double-membrane autophagosomes with partially digested cytoplasmic organelles were readily detectable in decorin-treated samples (arrows, Fig. 2 *C–E*). Quantification of three independent experiments showed an approximately fivefold increase in the number of autophagosomes per endothelial cell ($P < 0.001$) (Fig. 2*F*). Comparable qualitative and quantitative results were obtained with HUVEC (Fig. S2).

Decorin Induces Autophagy in Endothelial Cells, and This Process Is Blocked by 3-Methyladenine. We performed experiments to compare the activity of soluble decorin and that of rapamycin and 3-Methyladenine (3-MA). Rapamycin induces autophagy by inhibiting the mammalian target of rapamycin (mTOR) pathway, which antagonizes autophagy, whereas 3-MA inhibits autophagy by blocking the Class III PI3K human vacuolar protein sorting 34, necessary for autophagosome formation (32). We found that HUVEC exposed for 18 h to decorin (200 nM) contained a large number of Beclin 1/LC3-positive autophagosomes (white arrows,

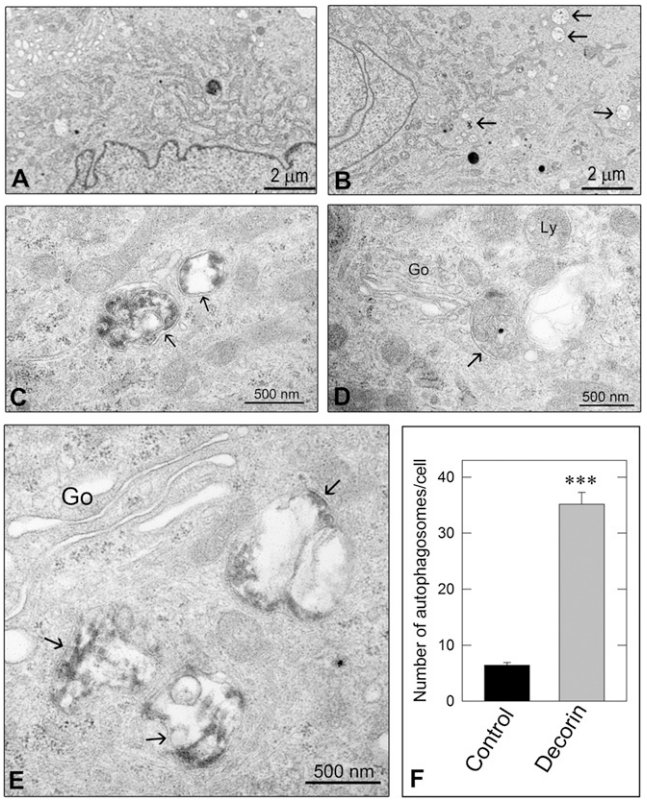

Fig. 2. Decorin induces autophagosomes in MDEC. (*A–E*) Gallery of transmission electron micrographs of MDEC following 18-h treatment with decorin (200 nM). Note the marked increase in the number of electron-dense vesicles (arrows in *B*) compared with vehicle-treated cells (*A*). Higher-magnification images of decorin-treated cells (*C–E*) show numerous double-membrane autophagosomes with partially digested cytoplasmic organelles (arrows); Go, Golgi; Ly, lysosome. (*F*) Quantification of three independent experiments shows approximately fivefold increase in the number of autophagosomes per endothelial cell in the decorin-treated cells (***$P < 0.001$). Comparable results were obtained with HUVEC (see Fig. S2).

Fig. 3*F*) similar to those induced in MDEC (see Fig. 1*H*). A comparable induction of autophagosome formation was obtained by rapamycin (20 nM) (Fig. 3*I*). 3-MA efficiently inhibited decorin-evoked formation of autophagosomes (Fig. 3*L*). Quantification of three experiments showed that decorin evoked a 4.8-fold increase in the average number of autophagosomes/cell ($P < 0.001$) (Fig. 3*M*), and this increase was blocked efficiently by 3-MA ($P < 0.001$) (Fig. 3*M*). These results indicate that decorin induces autophagy via the canonical PI3K/mTOR-dependent pathway.

Decorin Dynamically Regulates Beclin 1 and LC3 and Evokes Their Recruitment to Peg3. We investigated the temporal induction of Beclin 1 and LC3 by exogenous decorin in HUVEC. We found a rapid and sustained approximately threefold induction of Beclin 1, which peaked at 24 h and remained elevated up to 48 h (Fig. 3 *N* and *O*). LC3-I/II levels were elevated to a lesser degree, by ∼50% and 80%, respectively, at 12 h, and then both declined below basal levels by 24 and 48 h (Fig. 3 *N* and *O*). Notably, Beclin 1 levels were not affected by decorin in a variety of cancer cell lines including T47D, SKBR3, BT-20, and MDA-MB-231 breast carcinoma cells or in HeLa cells (Fig. S3*A*).

Next, we performed coimmunoprecipitation using anti-Peg3 and immunoblotting with antibodies directed to Peg3, Beclin 1, β-catenin, and LC3. We discovered that Beclin 1, β-catenin, and LC3 are recruited to decorin-induced Peg3 (Fig. 3*P*). Note that under basal conditions there already was an interaction between Peg3 and Beclin 1 but not between Peg3 and β-catenin or LC3. However, upon decorin treatment, there was a marked increase of these three proteins in the coimmunoprecipitates (Fig. 3*P*).

Collectively, these results indicate that decorin induces Peg3 and macroautophagy in normal endothelial cells but not in cancer cells, and this induction occurs via a dynamic modulation of the two key autophagic players, Beclin 1 and LC3, in addition to the established interaction with β-catenin.

Decorin Evokes Intracytoplasmic Colocalization of Peg3, Beclin 1, LC3, and β-Catenin. To corroborate further the coimmunoprecipitation studies described above, we used confocal microscopy with line scanning. The latter technique enumerates the number of pixels along a single axis in a specimen to resolve the localization of differentially labeled fluorophores (33, 34). The degree of overlap between interacting molecules provides a qualitative assessment of a proximity-dependent localization (35). Under basal conditions, Peg3 was not appreciably colocalized with Beclin 1, LC3, or β-catenin (Fig. 4 *A*, *C*, and *E*figE, respectively). In contrast, after a 6-h treatment with decorin there was extensive colocalization as shown by the overlapping of line-scanning profiles (Fig. 4 *B*, *D*, and *F*, respectively). Similar results were obtained with MDEC (Fig. S3 *B–E*). These findings corroborate the coimmunoprecipitation studies presented above.

Decorin Binds Directly and with High Affinity to the Ectodomain of VEGFR2. The finding that decorin induced autophagy selectively in endothelial cells but not in tumor cells led us to hypothesize that decorin could interact with an endothelial-specific receptor, i.e., VEGFR2, as previously demonstrated for extravillous trophoblasts (36). To this end, we performed solid-phase binding assays in which the seven Ig-like repeats of the human VEGFR2 ectodomain were used as immobilized substrate. We discovered that decorin bound with high affinity (K_d ∼2 nM) (Fig. 5*A*) to VEGFR2 ectodomain $Ig_{1–7}$. Moreover, immobilized decorin bound with similar affinity to soluble VEGFR2 $Ig_{1–7}$ (Fig. 5*B*), and its binding to VEGFR2 could be displaced efficiently by VEGFA (IC_{50} ∼50 nM) (Fig. 5*C*). Pull-down experiments revealed that recombinant VEGFR2 $Ig_{1–7}$ could be precipitated completely by decorin protein core-coated Ultralink beads (Fig. 5*D*). Collectively, our results demonstrate that decorin binds to the ectodomain of VEGFR2 in a region partially overlapping the natural ligand, VEGFA.

Decorin Requires VEGFR2 for Its Downstream Signaling and Transcriptional Regulation of VEGFA, Beclin 1, and LC3. To investigate decorin modulation of the VEGFA/VEGFR2 axis, we performed immunoblotting experiments in which HUVEC were treated with VEGFA (10 ng/mL) for 10 or 20 min with or without decorin (200 nM). In the latter case, HUVEC were preincubated with decorin for 10 min before the addition of VEGFA. The results showed that VEGFA induced robust phosphorylation of VEGFR2 at Tyr^{1175}, a key residue involved in activation of the receptor (37), and that decorin prevented VEGFR2 phosphorylation at this residue (Fig. 5*E*). We note that decorin did not cause any activation of VEGFR2 by itself. Thus, decorin could act as antagonist of VEGFR2 by binding to the ectodomain and preventing binding of its natural ligand VEGFA, thereby interfering with endothelial cell biology during tumor angiogenesis.

To corroborate the role of decorin in modulating the VEGFA/VEGFR2 axis, we used PAE-VEGFR2 cells stably expressing the luciferase gene under the control of the human *VEGFA* promoter (38, 39). We found that decorin induced a significant inhibition of *VEGFA* promoter luciferase activity within 6 h of treatment ($P < 0.001$) (Fig. 5*F*). Importantly, decorin evoked inhibitory activity similar to that of the VEGFR2 tyrosine kinase inhibitor SU5416 (40), and the combination of decorin and SU5416 did not evoke any further inhibition ($P < 0.001$) (Fig. 5*G*).

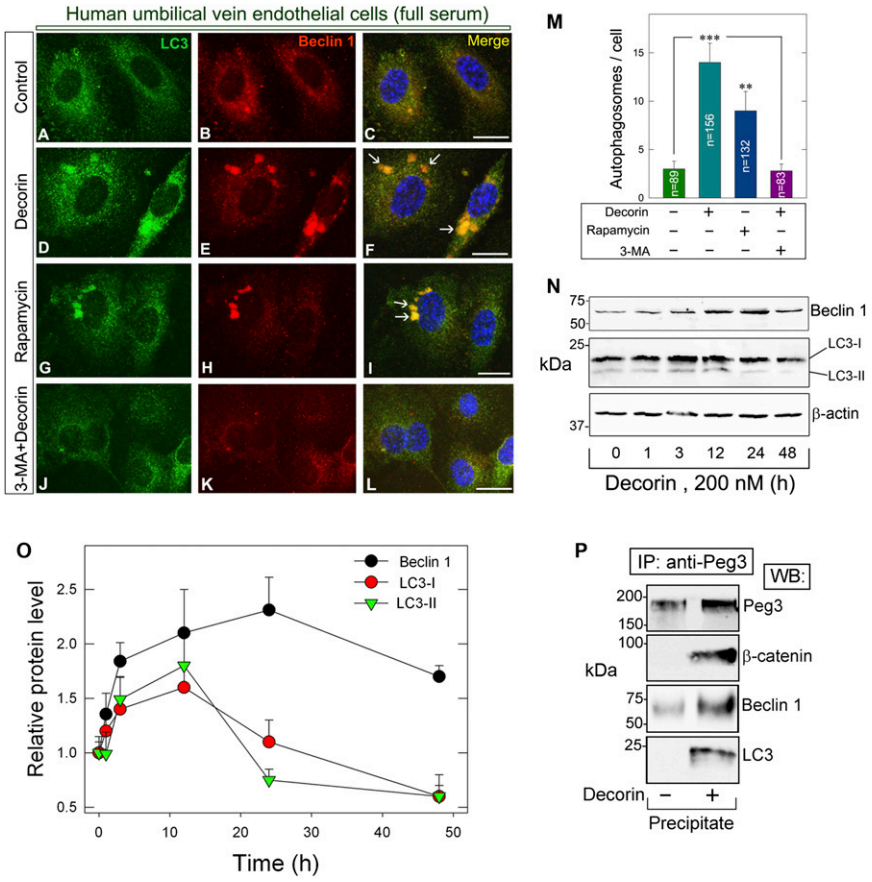

Fig. 3. Decorin induces expression and colocalization of the two autophagy markers LC3 and Beclin 1 and the interaction of these two proteins with Peg3. (*A–L*) Confocal analysis of HUVEC treated for 18 h with 200 nM decorin (*D–F*) or or 20 nM rapamycin(*G–I*) or preincubated with 5 mM 3-MA for 1 h before incubation with decorin(*J–L*). After treatment, cells were stained with specific antibodies against LC3 (green) and Beclin 1 (red). Nuclei were stained with DAPI. (Scale bars:~10 μm.) (*M*) Quantification of the number of autophagosomes per cells in HUVEC treated with 200 nM decorin or 20 nM rapamycin or pretreated with 5 mM 3-MA before decorin treatment. The graph is representative of four or five independent experiments in which 50 cells per field were counted. $^{**}P < 0.01$; $^{***}P < 0.001$. (*N*) Representative Western blot showing the time course of Beclin 1 and LC3-I/II expression in HUVEC upon stimulation with 200 nM decorin. β-Actin served as loading control. (*O*) Quantification of the relative protein levels of Beclin 1 and LC3-I/II from three independent experiments; data are shown as mean ± SEM. (*P*) Representative coimmunoprecipitation of MDEC stimulated with decorin (200 nM) for 6 h. The cells were lysed, immunoprecipitated (IP) with an anti-Peg3 antibody, and subjected to Western blotting with anti-Peg3, anti–β-catenin, anti-Beclin 1, and anti-LC3 as indicated. The experiments were repeated three times with comparable results.

Next, we profiled the effects of decorin on the transcriptional regulation of Beclin 1 (*BECN1*) and microtubule-associated protein 1 light chain 3 alpha (*MAPLC3A*) in HUVEC. We found a marked induction of both *BECN1* ($P < 0.001$) (Fig. 5*H*) and *MAPLC3A* ($P < 0.001$) (Fig. 5*I*) mRNA levels following exposure to either decorin or HBSS, which mimics nutrient deprivation. We note that decorin was used in nutrient-rich conditions, i.e., full serum. Decorin evoked a transcriptional response that was as strong as that seen with canonical nutrient depletion, e.g. with HBSS, and the effect was particularly apparent for *BECN1*. Because decorin rapidly evoked Peg3-dependent autophagy, we evaluated whether decorin induced mRNA stabilization for *PEG3*, *BECN1*, or *MAPLC3A*. We found that after 2-h exposure decorin evoked stability of *BECN1* and *MAPLC3A* in HUVEC, and similar results were obtained at 4 h as well (Fig. 5*J*). Interestingly, decorin did not stabilize *PEG3* mRNA (Fig. 5*J*).

Having established a decorin-evoked induction of autophagic gene transcription, we assessed the mRNA levels of *BECN1* and *MAPLC3A* following 6-h incubation with decorin, either alone or in combination with SU5416. We found a significant induction of both genes by decorin ($P < 0.001$) (Fig. 6 *A* and *B*) and that this induction could be blocked efficiently by SU5416 ($P < 0.01$) (Fig. 6 *A* and *B*). Similar results were obtained in MDEC for *Becn1* (Fig. 6*C*) and *Maplc3a* (Fig. 6*D*). In contrast to decorin, VEGFA was able to repress basal levels of *BECN1* mRNA significantly as well as abrogating decorin-evoked induction of *BECN1* mRNA (Fig. 6*E*). Importantly, coincubation with SU5416 completely abrogated decorin-evoked induction of Peg3 protein in HUVEC (Fig. S4*A*).

Next, we used siRNA specific for VEGFR2 and scrambled (Scr) siRNA. Decorin alone did not affect VEGFR2 mRNA levels. However, the siRNA for VEGFR2 was capable of reducing mRNA levels by ∼60% (Fig. 6*F*). Importantly, decorin-evoked transcriptional induction of *BECN1* and *MAPLC3A* could be blocked efficiently by the siRNA against VEGFR2 ($P < 0.001$ and $P < 0.5$, respectively) (Fig. 6 *G* and *H*).

To corroborate the transcriptional induction of *BECN1*, we stably transfected PAE-VEGFR2 cells with a luciferase reporter construct driven by a 645-bp fragment of the human *BECN1* promoter (41). We found that exposure of the PAE-VEGFR2$^{BECN1\text{-}Luc}$ cells to decorin (200 nM) caused a significant and rapid induction of luciferase activity which peaked at 1 h and remained elevated for up to 4 h (Fig. 6*I*). Luciferase activity was increased 10- to12-fold upon nutrient deprivation (in HBSS), indicating, in agreement with previous studies (41), that these reporter cells responded correctly to autophagic stimuli. Coincubation with SU5416 completely blocked the ability of decorin to induce *BECN1* promoter activity (Fig. 6*I*). We note that a recent study has identified a Peg3-specific DNA-binding motif (42), and indeed we found a single minimal consensus sequence for Peg3 (TGGCT) at −604 bp relative to the transcription start site. Collectively, these results support the notion that decorin signals through VEGFR2 in endothelial cells and corroborate the binding studies discussed above. Moreover, the binding of decorin to VEGFR2 is required for the transcriptional regulation of *BECN1* and *MAPLC3A*.

Peg3 Is Required for Decorin-Evoked Expression of the Autophagic Genes *Beclin 1* and *LC3*. Next, we investigated whether decorin required Peg3 to induce the transcription of Beclin 1 and LC3. To this end, we used either scrambled (Scr) siRNA or a mixture of validated siRNAs targeting Peg3. The latter significantly depleted Peg3 mRNA levels by ∼75% and ∼50% in MDEC and HUVEC, respectively (Fig. 7 *A* and *D*). Although the scrambled siRNA had no effect on the decorin-evoked induction of *BECN1* and *MAPLC3A* mRNA levels, siRNA-mediated depletion of

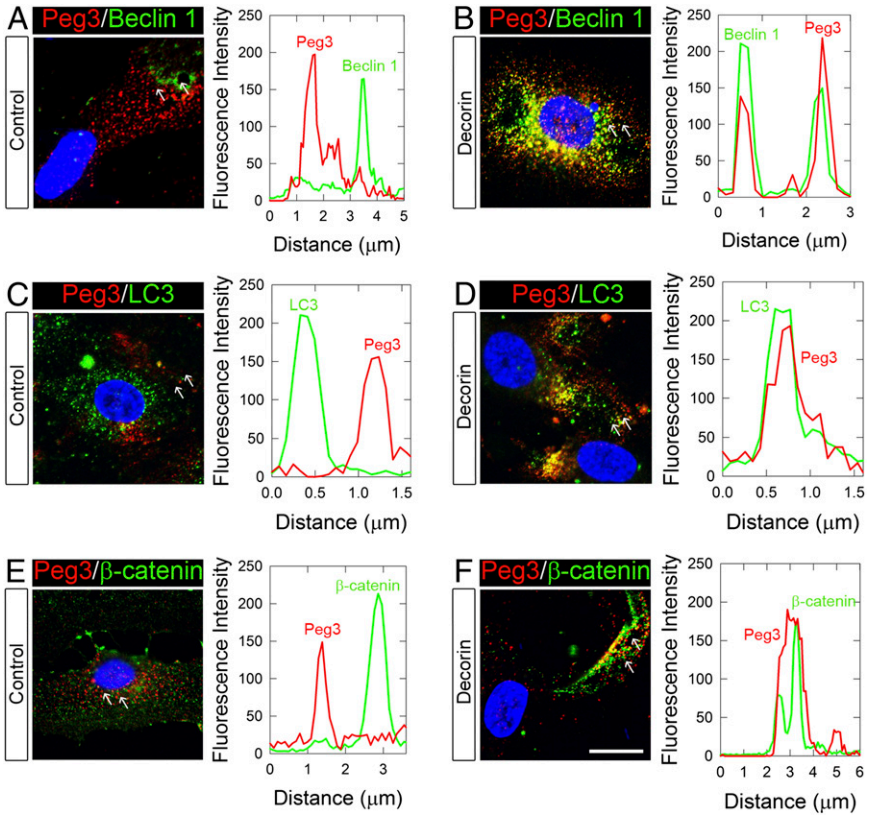

Fig. 4. Decorin induces colocalization of Peg3 with Beclin 1, LC3, and β-catenin. Representative confocal images of HUVEC following treatment with vehicle (control) or decorin (200 nM) for 6 h. The cells were permeabilized with 0.1% Triton X-100 for 1 min and were dually labeled for Peg3 (red) and Beclin 1 (green) (*A* and *B*), LC3 (green) (*C* and *D*), or β-catenin (green) (*E* and *F*). Nuclei appear blue after DAPI staining. All images were captured with the same exposure, gain, and intensity. The line-scanned profiles at the right of each confocal image show the distribution of fluorescence for each channel between the white arrows in the corresponding confocal images. (Scale bar: ~15 μm.)

Peg3 prevented the induction of both genes by decorin in MDEC (Fig. 7 *B* and *C*) and HUVEC (Fig. 7 *E* and *F*), respectively. We note that, especially in HUVEC, knockdown of Peg3 resulted in a significant reduction in basal levels of *BECN1* mRNA ($P < 0.001$) (Fig. 7*E*). Thus, decorin is capable of inducing the transcription of two key genes involved in autophagy, and this induction requires the upstream expression of Peg3.

We performed additional experiments to test the effects of siRNA-mediated Peg3 knockdown at the protein level. Again, decorin induced expression of Peg3 and Beclin 1 proteins in both MDEC (Fig. 7*G*) and HUVEC (Fig. 7*H*), and this induction could be blocked efficiently by the specific siRNA targeting Peg3. Moreover, the effects of rapamycin on Peg3 and Beclin 1 protein levels were similarly inhibited by the specific siRNA targeting Peg3 in MDEC (Fig. 7*G*) and HUVEC (Fig. 7*H*). Importantly, like decorin, rapamycin also induced Peg3 (Fig. S4*B*). Quantitative analysis of three independent experiments showed a significant block of Beclin 1 protein levels by siRNA-mediated depletion of Peg3 in both MDEC ($P < 0.01$) (Fig. S4*C*) and HUVEC ($P < 0.001$) (Fig. S4*D*). Collectively, these results indicate that Peg3 is a master regulator of autophagy downstream of the Class III PI3K/mTOR pathway and that Peg3 is required for decorin- and rapamycin-evoked induction of Beclin 1 at both the mRNA and protein level.

Decorin Induces GFP-LC3 and Inhibits Capillary Morphogenesis and Endothelial Cell Migration. To investigate further the role of decorin in inducing endothelial cell autophagy, we generated stable transfectants of PAE-VEGFR2 cells expressing LC3 tagged at the N terminus with GFP, allowing LC3 C-terminal lipidation and intercalation into autophagosome membranes. We discovered that 24-h exposure to either decorin (200 nM) or rapamycin (20 nM) evoked marked induction of GFP-LC3 (Fig. 8 *B* and *D*) as compared with cells exposed to either vehicle (Fig. 8*A*) or to equimolar concentrations of biglycan protein core (Fig. 8*C*). Induction of GFP-LC3 was observed as early as 2 h after exposure to recombinant decorin and peaked at 18–24 h. The effects of decorin were specific, in that the highly homologous biglycan was totally ineffective, even though it is ~60% identical to decorin as the evolutionarily closest SLRP (2).

Next, we tested whether decorin would inhibit capillary morphogenesis on Matrigel using the same stably transfected PAE cells as above. The results showed a marked inhibition of capillary morphogenesis by decorin (Fig. 8 *G–J*) *vis-á-vis* vehicle-treated cells (Fig. 8 *E* and *F*). Quantitative evaluation of capillary morphogenesis assays from several experiments revealed that the percentage of total area, the total tube number, the total tube length, and the total number of branching points were all significantly suppressed by exogenous decorin ($P < 0.001$) (Fig. 8*K*).

We then performed VEGFA-evoked endothelial cell migration assays through fibrillar collagen I-coated filters. The results showed a marked suppression of HUVEC migration by decorin (Fig. 8*M*), and this inhibition was highly significant ($P < 0.001$) (Fig. 8*N*). Thus, decorin concurrently induces autophagy and inhibits angiogenesis in endothelial cells.

Decorin Alters Mitochondrial Membrane Potential and Evokes Mitochondrial Fragmentation. Mitochondrial membrane potential, $\Delta\psi m$, is a key parameter of mitochondrial function (43). Therefore we assessed the effects of decorin on $\Delta\psi m$ using the mitochondrial dyes 5,5′,6,6′-tetrachloro-1,1′,3,3′ tetraethylbenzimidazol carbocyanine iodide (JC-1) and tetramethylrhodamine, ethyl ester (TMRE). JC-1 is a lipophilic, cationic dye that can enter mitochondria selectively and reversibly change color from green to red as the membrane potential increases. During high $\Delta\psi m$, as in healthy cells, JC-1 spontaneously forms complexes known as J-aggregates with intense red fluorescence (44). In contrast, in unhealthy cells with low $\Delta\psi m$, JC-1 retains its monomeric form that emits only green fluorescence. In live-cell microscopy, decorin caused a significant decrease in $\Delta\psi m$ (Fig. S5*B*). A loss of $\Delta\psi m$

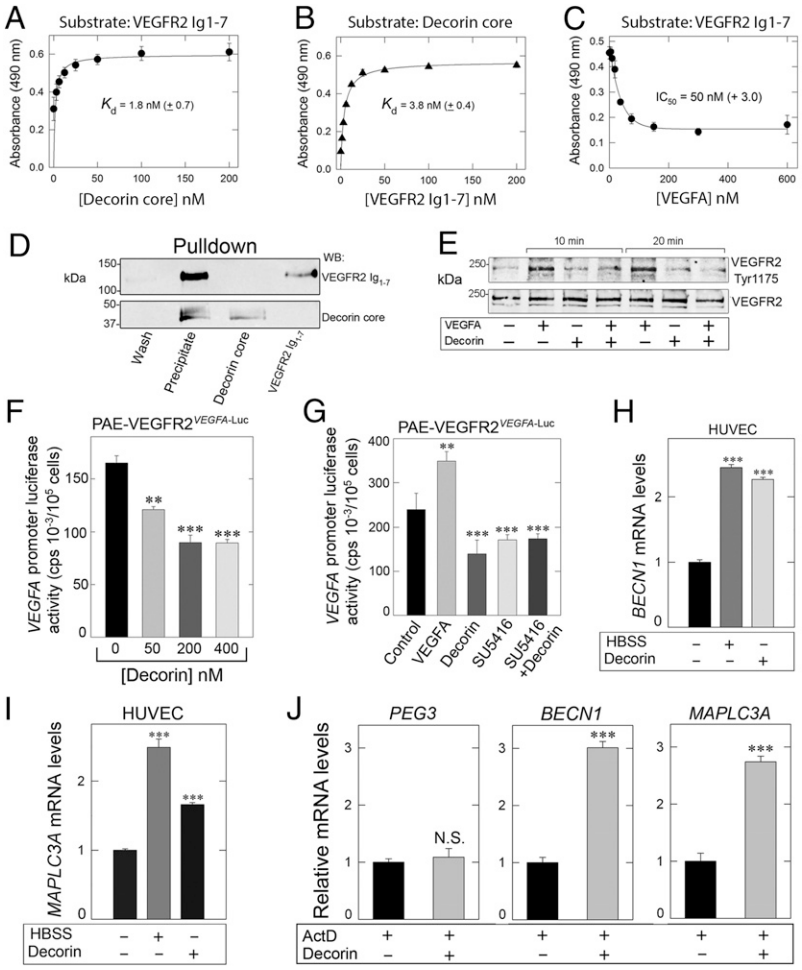

Fig. 5. Decorin requires VEGFR2 for its downstream signaling and transcriptional regulation of VEGFA, Beclin 1, and LC3. (*A* and *B*) Ligand-binding assays using decorin as the soluble ligand and the VEGFR2 Ig_{1-7} as the immobilized substrate, or vice versa, as indicated. Binding was recognized with either anti-decorin or anti-VEGFR2 antibody. Curves are nonlinear fits to a single-site binding equation as generated with the Systat software. (*C*) Displacement of VEGFR2-bound decorin (50 nM) using increasing molar concentrations of VEGFA. Data are shown as mean ± SEM; n = 3 experiments run in triplicate. (*D*) Representative Western blotting of VEGFR2 ectodomain and decorin after pull-down with UltraLink Biosupport beads-decorin. Positive controls for decorin and VEGFR2 Ig_{1-7} are shown in lanes 3 and 4, respectively. (*E*) Representative Western blot of HUVEC treated with VEGFA (10 ng/mL) or decorin (200 nM) for 10 or 20 min and immunoreacted with antibodies against VEGFR2-Tyr^{1175} or total VEGFR2. HUVEC were pretreated with decorin for 10 min before the addition of VEGFA. (*F*) Luciferase assays of PAE-VEGFR2$^{VEGFA\text{-}Luc}$ cells stably transfected with the promoter of VEGFA driving a luciferase reporter gene (39). The cells were exposed to increasing concentrations of decorin for 6 h. $^{**}P < 0.01$; $^{***}P < 0.001$. (*G*) Modulation of VEGFA promoter transcriptional activity following 6-h incubation with VEGFA (10 ng/mL), decorin (200 nM), SU5416 (30 μM), or decorin plus SU5416. Data are shown as mean ± SEM of three independent experiments; n = 6 for each condition. $^{**}P < 0.01$; $^{***}P < 0.001$. (*H* and *I*) Transcriptional induction of *BECN1* and *MAPLC3A* mRNA after 6-h exposure to decorin (200 nM) under nutrient-rich or nutrient-poor (HBSS) conditions. Data shown are mean ± SEM of three independent experiments run in quadruplicate. $^{***}P < 0.001$. (*J*) HUVEC mRNA stability assays evaluating *PEG3*, *BECN1*, and *MAPLC3A* via qPCR with 1-h pretreatment with Actinomycin D (ActD) (20 μg/mL) followed by 2-h exposure to decorin. Ct values, after normalization to *ACTB*, were subsequently normalized to a non-Actinomycin D control. Data shown are the mean fold change ± SEM of two independent experiments run in quadruplicate. $^{***}P < 0.001$.

also was seen at 24 h (Fig. S5*C*); however, there was partial recovery compared with the 6-h treatment. Notably, decorin was as effective as carbonylcyanide 4-triflouromethoxy phenylhydrazone (FCCP), a protonophore that rapidly (10 min) depolarizes the mitochondrial membranes (Fig. S5*D*). Quantification of three independent experiments showed a significant decorin-induced inhibition of Δψm, which also was highly significant at 24 h ($P < 0.001$) (Fig. S5*E*). These mitochondrial effects of decorin could be abolished completely by coincubation with SU5416 (Fig. S6*D*), further indicating that this bioactivity is mediated by the VEGFR2 signaling pathway.

Next, we tested the mitochondrial dye TMRE that emits red fluorescence in the presence of active mitochondria (Fig. S5*F*). Once again, upon treatment with decorin for 6 h there was a loss in Δψm as indicated by the loss of red fluorescence in live-cell microscopy (Fig. S5*G*). As with JC-1, there was a partial recovery at 24 h (Fig. S5*H*), although Δψm still was significantly down-regulated ($P < 0.001$) (Fig. S5*J*). Quantification of the TMRE data showed a pattern similar to that obtained with JC-1 (Fig. S5*J*). Collectively, these data indicate that decorin has the ability to cause depolarization of the mitochondrial membrane potential and that this effect requires active VEGFR2.

Having established a decorin-induced change in Δψm, we investigated whether decorin also could cause mitochondrial fragmentation. Using MitoTracker Deep Red dye which remains stable with minimal diffusion after fixation, we found that the tubular structure of mitochondria was prominent in control cells (Fig S6*E*), whereas decorin severely reduced mitochondrial size and disrupted mitochondrial architecture (Fig S6*F*). These results indicate that decorin tilts the mitochondrial dynamic balance toward fission in addition to decreasing Δψm, a process mediated by decorin/VEGFR2 interaction.

Discussion

The evolutionarily conserved eukaryotic process of autophagy promotes nonspecific turnover of bulk cytosolic components, long-lived proteins, and cellular organelles that have exceeded operational capacity or have become damaged (45). Autophagy can exert a potent oncosuppressive function by acting to discard critical organelles that otherwise would be involved in the promotion of the tumorigenic phenotype (46). This function is in perfect accordance with an emergent body of evidence that reinforces decorin as a soluble paracrine tumor repressor whose absence is permissive for tumorigenic growth. This activity is manifested through the concerted efforts to evoke intracellular degradation of several oncogenes downstream of receptor tyrosine kinase (RTK) signaling known to promote malignant conditions, including the myelocytomatosis viral oncogene homolog (Myc) and hypoxia-inducible factor alpha (5, 22, 23) as a molecular basis for angiostasis.

We hypothesized that decorin could down-regulate β-catenin by inducing expression of Peg3. Zebrafish embryos injected with Peg3 mRNA display marked defects in tail development (31). Similarly, injection of decorin in zebrafish embryos causes shortening of the body axis with defects in convergent extension (47) that are strikingly similar to those seen with injection of Peg3 mRNA. The noncanonical wingless-type MMTV integration site family (Wnt) pathway regulates convergent extension, because Wnt5 and Wnt11

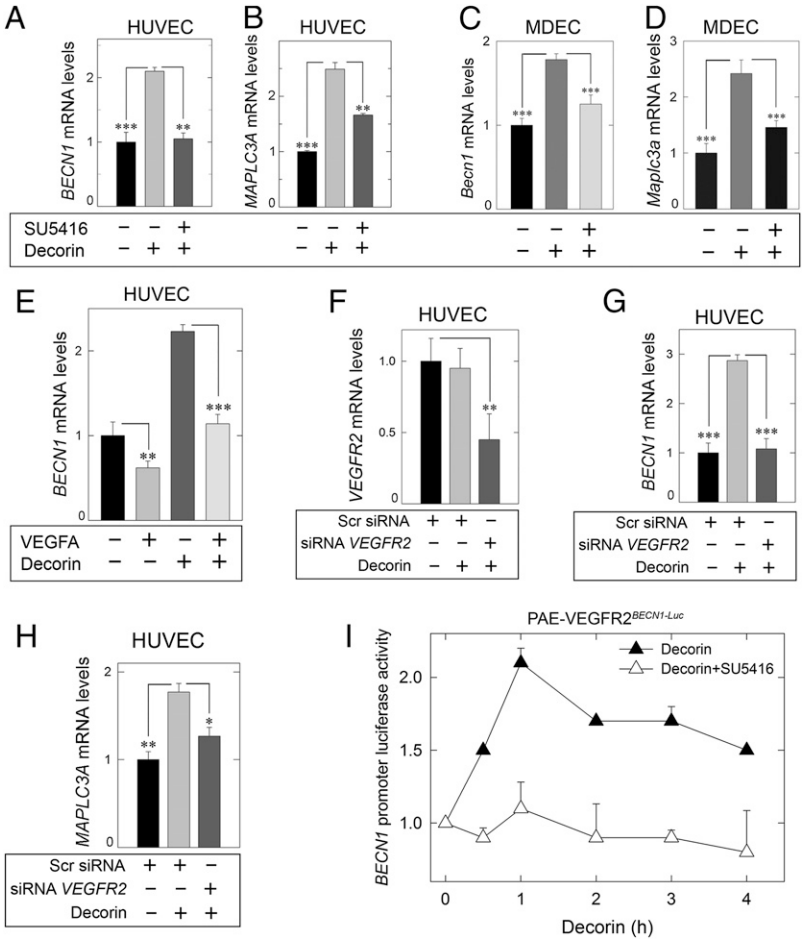

Fig. 6. Decorin requires VEGFR2 to induce mRNA expression of Beclin 1 in MDEC and HUVEC. (*A–D*) Effects of decorin (200 nM) ± SU5416 (30 μM) on the mRNA levels of *BECN1* and *MAPLC3A* normalized on *ACTB* mRNA in both HUVEC (*A* and *B*) and MDEC (*C* and *D*). Values represent the mean ± SEM of three independent experiments run in quadruplicate. $^{**}P < 0.01$; $^{***}P < 0.001$. (*E*) VEGFA (10 ng/mL) suppresses basal *BECN1* mRNA and is sufficient to block decorin-evoked transcriptional induction of *BECN1*. Values represent the mean ± SEM from three independent trials run in quadruplicate, normalized to *ACTB*. $^{**}P < 0.01$; $^{***}P < 0.001$. (*F–H*) Effects of siRNA directed toward VEGFR2 or scrambled (Scr) siRNA on the mRNA levels of VEGFR2 (*F*), *BECN1* (*G*), and *MAPLC3A* (*H*) in HUVEC. Cells were exposed to Scr siRNA or siRNA against VEGFR2 for 36 h and then were exposed to decorin for an additional 6 h. Data are shown as mean ± SEM of three independent experiments. $n = 4$ per condition, $^{*}P < 0.05$; $^{**}P < 0.01$; $^{***}P < 0.001$. (*I*) Luciferase reporter assays of PAE-VEGFR2$^{BECN1\text{-}Luc}$ cells exposed to 200 nM decorin for the designated times ± SU5416 (30 μM). Data are shown as mean ± SEM, normalized to total cell protein. All values are statistically significant with $P < 0.01$ compared with time 0 and with the SU5416-treated samples.

mutants show cyclopia and defects in convergent extension (48, 49). Thus, decorin and Peg3 are two key modulators of the noncanonical Wnt pathway in vertebrate development and possibly act within the same pathway during both developmental and tumorigenic processes. Notably, Wnt3a induces decorin expression in cocultures of hematopoietic stem progenitor and stromal cells (50). In this system, decorin causes changes similar to those caused by Wnt3a. Moreover, the number of hematopoietic stem cells is increased significantly in the bone marrow and spleen of decorin-null mice. Thus, decorin plays a key role in the mechanism of Wnt signaling and could shape niches supportive of hematopoiesis (50).

The first line of evidence to tie decorin signaling to Peg3 came from the empirical demonstration of Peg3 induction exclusively within the tumor microenvironment following systemic administration of decorin (24). Immunofluorescence studies revealed a dramatic association of Peg3 with subcellular structures resembling autophagosomes. The identity of these structures later was confirmed with prominent colocalization of the canonical autophagic markers Beclin 1 and LC3. Thus, we have linked a soluble constituent of the extracellular matrix to the intracellular digestive machinery in both macrovascular and microvascular endothelial cells.

The interaction discovered via confocal microscopy was corroborated by coimmunoprecipitation studies, which confirmed that Peg3 physically associates with Beclin 1 under basal conditions with further recruitment of LC3 and β-catenin in response to decorin. Collectively, these data implicate Peg3 as a putative component of the initial Beclin 1-containing autophagic scaffold, potentially integrating cellular bioenergetic inputs into autophagic outputs. Exogenous agents such as decorin engaging and signaling via VEGFR2 would further stimulate this association. We note that decorin-evoked autophagy in endothelial cells occurs under normoxia and nutrient-enriched conditions, suggesting a distinct pathway likely mediated by an antagonistic effect on the key angiogenic receptor VEGFR2. Furthermore, Peg3 also modulates LC3 in the later autophagic pathway but only after initiation of the process. In our current working model (Fig. S7) we postulate that decorin, by binding to VEGFR2, triggers a signaling cascade leading to induction of Class III PI3K and enhanced Peg3 stability and/or accumulation which in turn recruits Beclin 1, β-catenin, and LC3 to evoke autophagy. Decorin significantly stabilizes *BECN1* and *MAPLC3A* mRNA, but not *PEG3* mRNA, in HUVEC. Therefore enhanced Peg3 protein stability conceivably could orchestrate decorin-evoked autophagy via activation of *BECN1* and *MAPLC3A* expression. This process can be inhibited efficiently by depleting VEGFR2 with siRNA or pharmacologically blocking the VEGFR2 tyrosine kinase activity with the small molecule SU5416. It currently is unknown whether decorin triggers internalization of VEGFR2 in an analogous fashion to EGFR and Met, followed by lysosomal fusion and degradation. Further, it also remains to be shown whether decorin also cointernalizes with the targeted RTK; presumably decorin also is degraded by the lysosome following down-regulation. Decorin-induced Peg3 can transcriptionally enhance Beclin 1 and LC3, both of which can be blocked by Peg3 suppression via siRNA (Fig. S7). Thus, Peg3 can be considered a key protein in the initiation and maintenance of autophagy. Notably, Peg3 has been shown previously to be involved in regulation of cachexia (51), a severe muscle-wasting condition often associated with poor outcome in advanced cancer.

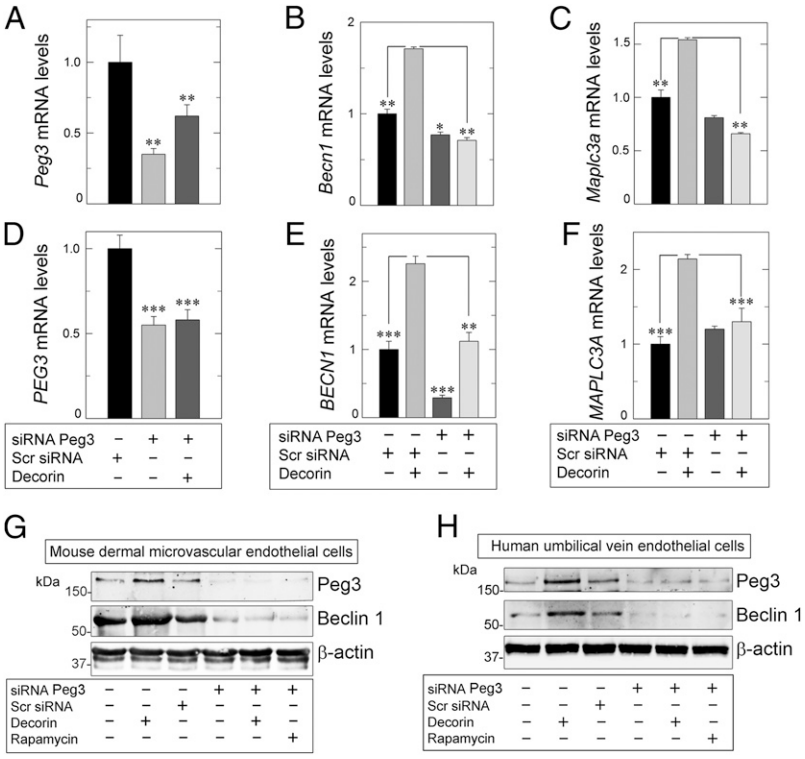

Fig. 7. Peg3 is required for decorin-evoked expression of the autophagic genes Beclin 1 and LC3 in MDEC and HUVEC. (*A* and *D*) Verification of Peg3 knockdown in MDEC (*A*) and HUVEC (*D*) after exposure to 200 nM decorin for 6 h in nutrient-rich medium relative to Scrambled (Scr) siRNA controls. (*B* and *E*) Loss of *Peg3* attenuates basal levels of *Becn1* mRNA and abrogates decorin-mediated induction of *Becn1* in MDEC (*B*) and HUVEC (*E*). (*C* and *F*) Although Peg3 is not required to maintain basal levels of *Maplc3a* in MDEC (*C*) and HUVEC (*F*), depletion of Peg3 does block decorin-evoked expression of *Maplc3a*. Data are shown ad mean ± SEM from three independent trials run in quadruplicate, normalized to *ACTB*. $*P < 0.05$; $**P < 0.01$; $***P < 0.001$. (*G* and *H*) Representative Western blot of MDEC (*G*) and HUVEC (*H*) after exposure to decorin (200 nM) or rapamycin (20 nM) for 6 h in nutrient-rich mediuim with or without specific siRNA targeting Peg3 or Scrambled siRNA. The data are representative of three experiments (see Fig. S4 *B* and *C*).

The functional role of Peg3 was proven to be indispensable not only for decorin-evoked autophagy, as signified by induction of Beclin 1, but also for maintaining basal levels of Beclin 1. Indeed, siRNA-mediated silencing of Peg3 substantially reduces basal levels of Beclin 1 mRNA and protein, most prominently in HUVEC. However, this effect is not achieved in MDEC. This difference might result from inherent differences in these primary cells, in that HUVEC are more embryonic than MDEC and thus might be more attuned to the function of Peg3, recently characterized as a candidate stem cell marker (52). Intriguingly, basal levels of *MAPLC3A* are relatively unperturbed by Peg3 silencing. However, in both MDEC and HUVEC, silencing of Peg3 severely compromises decorin-dependent induction of *BECN1* and *MAPLC3A* expression. These effects are mirrored at the protein level, thereby indicating that Peg3 has a vital transcriptional function over these critical autophagic targets. Further, Peg3 is wholly responsible for decorin-mediated induction of Beclin 1 and thus decorin-evoked endothelial cell autophagy. Importantly, loss of Peg3 via siRNA also prevents rapamycin from inducing Beclin1 and LC3. This result provides insight into the upstream regulation of Peg3, because rapamycin potently inhibits mTOR.

We should point out that when the decorin proteoglycan was used, we obtained comparable results, indicating that the glycosaminoglycan chain is dispensable. Specificity was confirmed by the lack of an autophagic response in the presence of equimolar amounts of biglycan protein core, the closest molecular relative of decorin. Decorin, by signaling via RTK interactions, can ameliorate the overall antitumor properties of the tumor stroma by counteracting malignant development to stymie tumor progression (5, 13, 24) and angiogenesis (20, 23). Typically, these interactions are exclusively antagonistic. However, in HUVEC and MDEC, incubation with SU5416 completely abrogates decorin-dependent induction of *BECN1* and *MAPLC3A* expression. This effect is further confirmed with siRNA targeting VEGFR2 in HUVEC, which phenocopy the results obtained with SU5416. Pretreatment of HUVEC with VEGFA completely abrogates the ability of decorin to induce transcriptional activation of *BECN1*, whereas VEGFA alone is sufficient to evoke suppression of basal *BECN1* mRNA. These data confirm not only that VEGFR2 is required but also that decorin must signal through this RTK to achieve transcriptional activation of the target loci, in a mechanism inherently different from that of VEGFA. Moreover, VEGFR2 lies upstream of Peg3, because these data are entirely epistatic to the depletion of Peg3 and the ensuing effects on decorin-evoked expression of *BECN1* and *MAPLC3A*.

Decorin can signal through the EGFR and induce rapid thrombospondin-1 secretion from the tumor parenchyma and mammary carcinoma cells (53). This signaling could represent an additional anti-angiogenic activity of this molecule that could modulate the biology of several types of cancer by directly affecting the tumor microenvironment (54, 55). Moreover, we have shown previously that there is a genetic cooperation between decorin and p53, because double-null mice succumb to a highly aggressive thymic lymphoma within the first 6 mo of postnatal life, whereas p53-null mice live longer and present several types of neoplasia (56). Notably, Peg3 has been shown to regulate p53-mediated apoptosis by interacting directly with the Seven in absentia homolog 1 (Siah1a) (57) and by inducing Bcl2-associated X (Bax) translocation from the cytosol to mitochondria (58). Thus, it is plausible that decorin might affect this pathway in endothelial cells also, because we have shown previously that decorin induces apoptosis in carcinoma cells by activating caspase 3 (59).

The functional consequences of Beclin 1 induction being dependent on VEGFR2 and Peg3 regulation could be important for blunting capillary morphogenesis, restricting endothelial cell migration, and compromising mitochondrial membrane integrity. This scenario is further supported by the loss of $\Delta\psi m$, typically an early harbinger of the intrinsic apoptotic response (43). However, this function also may activate autophagy as a mechanism to eliminate damaged mitochondria in an attempt to save the cell from the damaging effects of reactive oxygen species and ensuing peroxidative stressors, leading to further mutagenic events that foster tumorigenesis. The induction of endothelial cell autophagy in the light of inhibited capillary morphogenesis might be func-

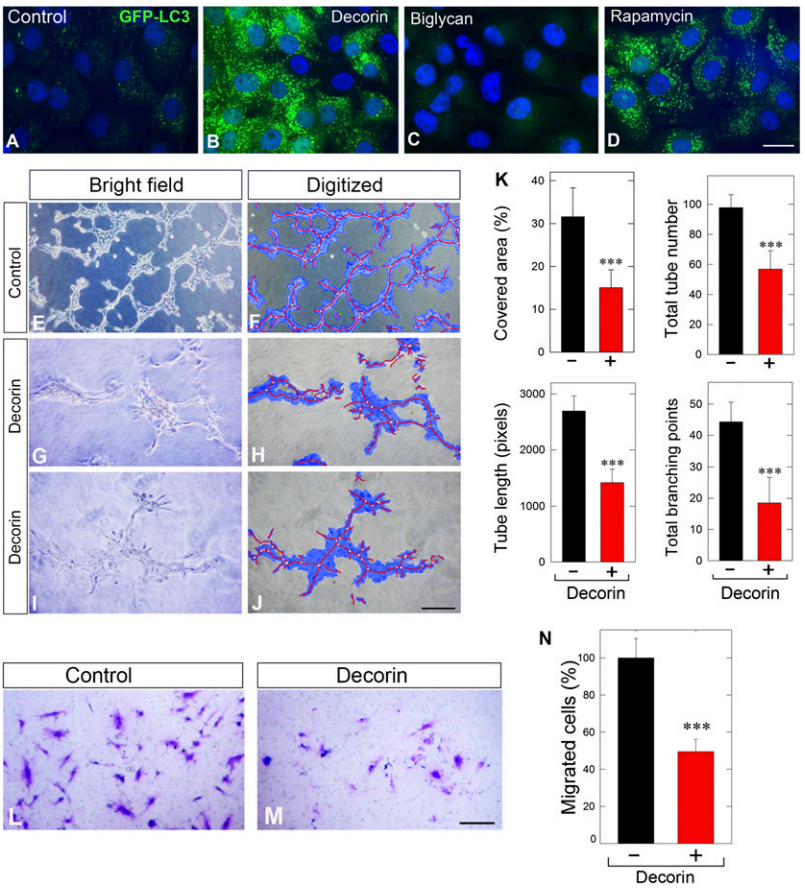

Fig. 8. Decorin induces GFP-LC3 and inhibits capillary morphogenesis and migration through fibrillar collagen. (*A–D*) Representative fluorescence micrographs of PAE cells stably transfected with GFP-LC3 and treated for 24 h with decorin (200 nM), biglycan protein core (200 nM), rapamycin (20 nM), or vehicle as indicated. All images were taken with the same exposure (500 ms), intensity (set at 5), and gain (set at 4). Nuclei are stained in blue (DAPI). (Scale bar: ∼15 μm.) (*E–J*) Representative micrographs of PAE-GFP-LC3 cells forming capillary morphogenesis on Matrigel. The cells were seeded on growth factor-depleted Matrigel-coated wells supplemented with VEGFA (40 ng/mL) and heparin (50 nM) with or without decorin (200 nM). *E*, *G*, and *I* are bright field images. *F*, *H*, and *J* are digitized images used for quantification. (Scale bar: ∼100 μm.) (*K*) Quantitative evaluation of capillary morphogenesis assays from several experiments shown in *E–J*. ***$P < 0.001$. Images were acquired and quantified after 5–6 h of stimulation. (*L* and *M*) Representative images of VEGFA-evoked migration of HUVEC. The images were captured from the bottom of the collagen I-coated filter after a 4-h migration. (*N*) Quantification of HUVEC migration through fibrillar collagen I as evoked by VEGFA (40 ng/mL in the lower chamber). Data are shown as mean ± SEM of three independent experiments run in triplicate. ***$P < 0.001$.

tionally linked via Peg3, a master regulator of macroautophagy. The requirement of decorin-mediated autophagy within the stroma might form the fundamental basis for decorin-dependent angiostasis and therefore underlies the basic tumoricidal properties of the molecule.

In conclusion, our studies delineate a key role for soluble decorin in reprogramming the tumor stroma via direct induction of endothelial cell autophagy, a fundamental cellular process that in this context acts to combat tumor angiogenesis. The discovery that decorin-induced Peg3 is competent to activate the transcription of autophagic proteins such as Beclin 1 and LC3 indicates that messages embedded in the extracellular milieu can profoundly affect autophagy. These data further stress the need for treatment based on systemic delivery of decorin, a genuinely multifaceted matrix constituent, as a viable modality in the ongoing war against cancer.

Materials and Methods

A detailed description of materials, protocols for immunofluorescence, confocal microscopy, siRNA-mediated silencing, quantitative PCR, migration and pull down assays, and mitochondrial membrane potential analysis can be found in *SI Materials and Methods*. PAE cells and their transgenic counterparts were described previously (60). Decorin was purified as described previously (61).

ACKNOWLEDGMENTS. We thank Dr. S. Ramakrishnan for providing the GFP-LC3 plasmid, Dr. H. Rui for providing some of the breast carcinoma cells, Dr. L. Claesson-Welsh for generously providing the PAE-VEGFR2 cells, and Dr. F. Demarchi for providing the *BECN1* promoter-luciferase construct. This work was supported in part by National Institutes of Health (NIH) Grants R01 CA39481, R01 CA47282, and R01 CA120975 (to R.V.I.). T.N. was supported by NIH Training Grant T32 AA07463. A.T. was supported by a Diversity Research Supplement NIH Grant CA39481-26S1. This work is a partial fulfillment of T.N,'s and A.T.'s doctoral theses in Cell and Developmental Biology, Thomas Jefferson University.

1. Bissell MJ, Hines WC (2011) Why don't we get more cancer? A proposed role of the microenvironment in restraining cancer progression. *Nat Med* 17(3):320–329.
2. Iozzo RV, Goldoni S, Berendsen A, Young MF (2011) *Extracellular Matrix: An Overview*, ed Mecham RP (Springer, Berlin), pp 197–231.
3. Schaefer L, Iozzo RV (2008) Biological functions of the small leucine-rich proteoglycans: From genetics to signal transduction. *J Biol Chem* 283(31):21305–21309.
4. Iozzo RV, Schaefer L (2010) Proteoglycans in health and disease: Novel regulatory signaling mechanisms evoked by the small leucine-rich proteoglycans. *FEBS J* 277(19): 3864–3875.
5. Schaefer L, Iozzo RV (2012) Small leucine-rich proteoglycans, at the crossroad of cancer growth and inflammation. *Curr Opin Genet Dev* 22(1):56–57.
6. Bolton K, et al. (2008) Decorin is a secreted protein associated with obesity and type 2 diabetes. *Int J Obes (Lond)* 32(7):1113–1121.
7. Merline R, et al. (2011) Signaling by the matrix proteoglycan decorin controls inflammation and cancer through PDCD4 and MicroRNA-21. *Sci Signal* 4(199):ra75.
8. Xu Y-Z, et al. (2012) Dynamic reduction of plasma decorin following ischemic stroke: A pilot study. *Neurochem Res* 37(9):1843–1848.
9. Wu I-C, et al. (2010) Plasma decorin predicts the presence of esophageal squamous cell carcinoma. *Int J Cancer* 127(9):2138–2146.
10. Goldoni S, et al. (2004) Biologically active decorin is a monomer in solution. *J Biol Chem* 279(8):6606–6612.
11. Iozzo RV, Moscatello DK, McQuillan DJ, Eichstetter I (1999) Decorin is a biological ligand for the epidermal growth factor receptor. *J Biol Chem* 274(8):4489–4492.
12. Goldoni S, et al. (2009) Decorin is a novel antagonistic ligand of the Met receptor. *J Cell Biol* 185(4):743–754.
13. Iozzo RV, et al. (2011) Decorin antagonizes IGF receptor I (IGF-IR) function by interfering with IGF-IR activity and attenuating downstream signaling. *J Biol Chem* 286(40):34712–34721.
14. Baghy K, et al. (2013) Decorin interferes with platelet-derived growth factor receptor signaling in experimental hepatocarcinogenesis. *FEBS J* 280(10):2150–2164.
15. Morrione A, Neill T, Iozzo RV (2013) Dichotomy of decorin activity on the insulin-like growth factor-I system. *FEBS J* 280(10):2138–2149.
16. Neill T, Schaefer L, Iozzo RV (2012) Decorin: A guardian from the matrix. *Am J Pathol* 181(2):380–387.

17. Reed CC, Gauldie J, Iozzo RV (2002) Suppression of tumorigenicity by adenovirus-mediated gene transfer of decorin. *Oncogene* 21(23):3688–3695.
18. Tralhão JG, et al. (2003) In vivo selective and distant killing of cancer cells using adenovirus-mediated decorin gene transfer. *FASEB J* 17(3):464–466.
19. Reed CC, et al. (2005) Decorin prevents metastatic spreading of breast cancer. *Oncogene* 24(6):1104–1110.
20. Grant DS, et al. (2002) Decorin suppresses tumor cell-mediated angiogenesis. *Oncogene* 21(31):4765–4777.
21. Goldoni S, et al. (2008) An antimetastatic role for decorin in breast cancer. *Am J Pathol* 173(3):844–855.
22. Buraschi S, et al. (2010) Decorin antagonizes Met receptor activity and down-regulates β-catenin and Myc levels. *J Biol Chem* 285(53):42075–42085.
23. Neill T, et al. (2012) Decorin antagonizes the angiogenic network: Concurrent inhibition of Met, hypoxia inducible factor 1α, vascular endothelial growth factor A, and induction of thrombospondin-1 and TIMP3. *J Biol Chem* 287(8):5492–5506.
24. Buraschi S, et al. (2012) Decorin protein core affects the global gene expression profile of the tumor microenvironment in a triple-negative orthotopic breast carcinoma xenograft model. *PLoS ONE* 7(9):e45559.
25. Maegawa S, et al. (2001) Epigenetic silencing of PEG3 gene expression in human glioma cell lines. *Mol Carcinog* 31(1):1–9.
26. Feng W, et al. (2008) Imprinted tumor suppressor genes *ARHI* and *PEG3* are the most frequently down-regulated in human ovarian cancers by loss of heterozygosity and promoter methylation. *Cancer* 112(7):1489–1502.
27. Kohda T, et al. (2001) Tumour suppressor activity of human imprinted gene *PEG3* in a glioma cell line. *Genes Cells* 6(3):237–247.
28. Dowdy SC, et al. (2005) Biallelic methylation and silencing of paternally expressed gene 3 (*PEG3*) in gynecologic cancer cell lines. *Gynecol Oncol* 99(1):126–134.
29. Zhai Y, et al. (2010) Loss of estrogen receptor 1 enhances cervical cancer invasion. *Am J Pathol* 177(2):884–895.
30. Gloss BS, et al. (2012) Integrative genome-wide expression and promoter DNA methylation profiling identifies a potential novel panel of ovarian cancer epigenetic biomarkers. *Cancer Lett* 318(1):76–85.
31. Jiang X, et al. (2010) The imprinted gene *PEG3* inhibits Wnt signaling and regulates glioma growth. *J Biol Chem* 285(11):8472–8480.
32. Mizushima N, Yoshimori T, Levine B (2010) Methods in mammalian autophagy research. *Cell* 140(3):313–326.
33. Thurston TLM, Wandel MP, von Muhlinen N, Foeglein A, Randow F (2012) Galectin 8 targets damaged vesicles for autophagy to defend cells against bacterial invasion. *Nature* 482(7385):414–418.
34. Sai J, Raman D, Liu Y, Wikswo J, Richmond A (2008) Parallel phosphatidylinositol 3-kinase (PI3K)-dependent and Src-dependent pathways lead to CXCL8-mediated Rac2 activation and chemotaxis. *J Biol Chem* 283(39):26538–26547.
35. Molinaro P, et al. (2011) Na^+ -Ca^{2+} exchanger (NCX3) knock-out mice display an impairment in hippocampal long-term potentiation and spatial learning and memory. *J Neurosci* 31(20):7312–7321.
36. Khan GA, Girish GV, Lala N, Di Guglielmo GM, Lala PK (2011) Decorin is a novel VEGFR-2-binding antagonist for the human extravillous trophoblast. *Mol Endocrinol* 25(8):1431–1443.
37. Koch S, Tugues S, Li X, Gualandi L, Claesson-Welsh L (2011) Signal transduction by vascular endothelial growth factor receptors. *Biochem J* 437(2):169–183.
38. Goyal A, et al. (2011) Endorepellin, the angiostatic module of perlecan, interacts with both the α2β1 integrin and vascular endothelial growth factor receptor 2 (VEGFR2): A dual receptor antagonism. *J Biol Chem* 286(29):25947–25962.
39. Goyal A, et al. (2012) Endorepellin affects angiogenesis by antagonizing diverse VEGFR2- evoked signaling pathways: Transcriptional repression of HIF-1α and VEGFA and concurrent inhibition of NFAT1 activation. *J Biol Chem* 287:43543–43556.
40. Fong TAT, et al. (1999) SU5416 is a potent and selective inhibitor of the vascular endothelial growth factor receptor (Flk-1/KDR) that inhibits tyrosine kinase catalysis, tumor vascularization, and growth of multiple tumor types. *Cancer Res* 59(1):99–106.
41. Copetti T, Bertoli C, Dalla E, Demarchi F, Schneider C (2009) p65/RelA modulates *BECN1* transcription and autophagy. *Mol Cell Biol* 29(10):2594–2608.
42. Thiaville MM, et al. (2013) DNA-binding motif and target genes of the imprinted transcription factor PEG3. *Gene* 512(2):314–320.
43. Kirkin V, McEwan DG, Novak I, Dikic I (2009) A role for ubiquitin in selective autophagy. *Mol Cell* 34(3):259–269.
44. Cossarizza A, Baccarani-Contri M, Kalashnikova G, Franceschi C (1993) A new method for the cytofluorimetric analysis of mitochondrial membrane potential using the J-aggregate forming lipophilic cation 5,5′,6,6′-tetrachloro-1,1′,3,3′-tetraethylbenzimidazolcarbocyanine iodide (JC-1). *Biochem Biophys Res Commun* 197(1):40–45.
45. Mizushima N, Komatsu M (2011) Autophagy: Renovation of cells and tissues. *Cell* 147 (4):728–741.
46. White E (2012) Deconvoluting the context-dependent role for autophagy in cancer. *Nat Rev Cancer* 12(6):401–410.
47. Zoeller JJ, et al. (2009) A central role for decorin during vertebrate convergent extension. *J Biol Chem* 284(17):11728–11737.
48. Heisenberg C-P, et al. (2000) Silberblick/Wnt11 mediates convergent extension movements during zebrafish gastrulation. *Nature* 405(6782):76–81.
49. Hammerschmidt M, et al. (1996) Mutations affecting morphogenesis during gastrulation and tail formation in the zebrafish, Danio rerio. *Development* 123: 143–151.
50. Ichii M, Frank MB, Iozzo RV, Kincade PW (2012) The canonical Wnt pathway shapes niches supportive of hematopoietic stem/progenitor cells. *Blood* 119(7):1683–1692.
51. Schwarzkopf M, Coletti D, Sassoon D, Marazzi G (2006) Muscle cachexia is regulated by a p53-PW1/Peg3-dependent pathway. *Genes Dev* 20(24):3440–3452.
52. Besson V, et al. (2011) *PW1* gene/paternally expressed gene 3 (PW1/Peg3) identifies multiple adult stem and progenitor cell populations. *Proc Natl Acad Sci USA* 108(28): 11470–11475.
53. Neill T, et al. (2013) Decorin induces rapid secretion of thrombospondin-1 in basal breast carcinoma cells via inhibition of Ras homolog gene family, member A/Rho-associated coiled-coil containing protein kinase 1. *FEBS J* 280(10):2353–2368.
54. Goldoni S, Iozzo RV (2008) Tumor microenvironment: Modulation by decorin and related molecules harboring leucine-rich tandem motifs. *Int J Cancer* 123(11): 2473–2479.
55. Iozzo RV, Sanderson RD (2011) Proteoglycans in cancer biology, tumour microenvironment and angiogenesis. *J Cell Mol Med* 15(5):1013–1031.
56. Iozzo RV, et al. (1999) Cooperative action of germ-line mutations in decorin and p53 accelerates lymphoma tumorigenesis. *Proc Natl Acad Sci USA* 96(6):3092–3097.
57. Relaix F, et al. (2000) Pw1/Peg3 is a potential cell death mediator and cooperates with Siah1a in p53-mediated apoptosis. *Proc Natl Acad Sci USA* 97(5):2105–2110.
58. Deng Y, Wu X (2000) Peg3/Pw1 promotes p53-mediated apoptosis by inducing Bax translocation from cytosol to mitochondria. *Proc Natl Acad Sci USA* 97(22): 12050–12055.
59. Seidler DG, et al. (2006) Decorin protein core inhibits *in vivo* cancer growth and metabolism by hindering epidermal growth factor receptor function and triggering apoptosis via caspase-3 activation. *J Biol Chem* 281(36):26408–26418.
60. Waltenberger J, Claesson-Welsh L, Siegbahn A, Shibuya M, Heldin CH (1994) Different signal transduction properties of KDR and Flt1, two receptors for vascular endothelial growth factor. *J Biol Chem* 269(43):26988–26995.
61. Zhu J-X, et al. (2005) Decorin evokes protracted internalization and degradation of the EGF receptor via caveolar endocytosis. *J Biol Chem* 280:32468–32479.